NMR determination of noncollinear antiferromagnetic structure in $TbCoGa_5$

Yo Tokunaga,[1,*] Yo Saito,[1,2] Hironori Sakai,[1] Shinsaku Kambe,[1] Naoyuki Sanada,[3] Ryuta Watanuki,[3] Kazuya Suzuki,[3] Yu Kawasaki,[2] and Yutaka Kishimoto[2]

[1]*Advanced Science Research Center, Japan Atomic Energy Agency, Tokai, Ibaraki 319-1195, Japan*

[2]*Department of Advanced Materials, Institute of Technology and Science, The University of Tokushima, Tokushima 770-8506, Japan*

[3]*Department of Advanced Materials Chemistry, Yokohama National University, Yokohama 240-8501, Japan*

(Received 5 September 2011; revised manuscript received 9 November 2011; published 2 December 2011)

We report NMR studies of $TbCoGa_5$, which has the tetragonal $HoCoGa_5$ structure and exhibits two antiferromagnetic (AF) transitions at $T_{N1} = 36.2$ K and $T_{N2} = 5.4$ K. From a symmetry analysis of internal magnetic fields at orthorhombic Ga sites, we have successfully determined the magnetic structures in the AF-I ($T_{N2} < T < T_{N1}$) and AF-II ($T < T_{N2}$) phases. The AF-I phase is a collinear AF order with a propagation vector $\boldsymbol{q} = [1/2,0,1/2]$ and ordered moments parallel to the [001] direction. In the AF-II phase, on the other hand, we found a noncollinear AF structure described by double propagation vectors $\boldsymbol{q_1} = [1/2,0,1/2]$ and $\boldsymbol{q_2} = [0,1/2,1/2]$, where the moments tilt away from the [001] direction toward [100], keeping a constant value along the [001] direction. In the context of these results, we discuss the possible presence of magnetic frustration in this system.

DOI: 10.1103/PhysRevB.84.214403 PACS number(s): 75.25.−j, 75.50.Ee, 76.60.Jx

I. INTRODUCTION

Intensive studies have been performed on compounds with the tetragonal $HoCoGa_5$-type structure (the so-called 115 systems) over the past few decades.[1] Although this research was stimulated initially by the discovery of unconventional superconductivity in Ce- and Pu-based compounds,[2–5] the richness of their magnetic behavior has also attracted considerable attention. The interplay between superconductivity and magnetism is a central issue in studies of the 115 systems.

$TbCoGa_5$ has recently been reported to exhibit two successive magnetic transitions, at $T_{N1} = 36.2$ K and at $T_{N2} = 5.4$ K.[6] This compound also possesses the 115 structure, as shown in Fig. 1.[7] The susceptibility along the c direction exhibits a clear peak at T_{N1}, while the susceptibility along the a direction increases progressively with decreasing temperature below T_{N1}, showing a rather sharp peak at T_{N2}.[8,9] Magnetic entropy data suggest that the degeneracy of internal degrees of freedom is not fully lifted above T_{N2}. Thus the compound has been proposed to exhibit successive "components-separated"antiferromagnetic (AF) transitions, where the c components of the Tb magnetic moments order at T_{N1}, while the a components order only at T_{N2}.[8,9]

Neutron-diffraction (ND) measurements have also been performed recently on a powder sample of $TbCoGa_5$.[10] Based on ND data, the propagation vector $\boldsymbol{q} = \langle 1/2,0,1/2\rangle$ has been deduced for both the AF-I ($T_{N2} < T < T_{N1}$) and AF-II ($T < T_{N2}$) phases. Rietveld analysis has suggested that ordered magnetic moments lie parallel to the c axis, with a magnetic moment value of 8.32 μ_B for the AF-I phase, which is 92.4% of the full moment of the Tb^{3+} ion. For the AF-II phase, four possible models of magnetic structure, two collinear and two noncollinear, have been proposed. However, these four structural models are not distinguishable, in principle, by means of ND data alone, because of the tetragonal symmetry of the crystal.

In this work, we have performed ^{69,71}Ga antiferromagnetic nuclear magnetic resonance (AFNMR) under zero magnetic field. From a symmetry analysis of internal magnetic fields induced by the ordered Tb moments at orthorhombic Ga sites, we have determined magnetic structures in both the AF-I and the AF-II phases. We have confirmed a collinear structure proposed on the basis of ND measurements in the AF-I phase. On the other hand, for the AF-II phase, we have found a noncollinear structure described with two different propagation vectors. Based on these results, we then proceed to discuss magnetic interactions in this system.

II. EXPERIMENTAL RESULTS

Single crystals of $TbCoGa_5$ were grown by the self-flux method. Details of sample preparation are given elsewhere.[9] The AFNMR measurements have been performed using several small pieces of single crystal. The frequency-swept AFNMR spectra were obtained by stepwise summing of the spin-echo signal intensity, using a conventional pulsed spectrometer with an autotuning NMR probe.

In the 115 structure ($P4/mmm$), there are two inequivalent Ga sites, Ga1 (1c site) and Ga2 (4i site). The internal field on the Ga1 is canceled for the in-plane propagation vector of the AF arrangement. In this study, we focus on the Ga2 site with orthorhombic symmetry. Nuclear gyromagnetic ratio values are $^{69}\gamma_N/2\pi = 1.0220$ MHz/kOe and $^{71}\gamma_N/2\pi = 1.29855$ MHz/kOe for ^{69}Ga and ^{71}Ga nuclei, respectively. Both Ga nuclei have a nuclear spin $I = 3/2$ larger than 1/2, so there are nuclear quadrupolar interactions. The directions of their electric-field-gradient (EFG) tensor principal axes X, Y, and Z are shown in Fig. 1. These were deduced by analogy with other 115 compounds,[11,12] and were also confirmed experimentally with NMR under external field, as is described later. The EFG components V_{XX}, V_{YY}, and V_{ZZ} obey the relations $V_{ZZ} > V_{YY} > V_{XX}$ and $V_{ZZ} + V_{YY} + V_{XX} = 0$. The asymmetry parameter η is defined as $\eta = (V_{XX} - V_{YY})/V_{ZZ}$.

Figure 2 shows the frequency-swept AFNMR spectrum obtained at 9 K (the AF-I phase). Arrows indicate the peaks arising from the Ga2 sites of $TbCoGa_5$. These peaks have extremely short T_2 and thus disappear when we used τ of

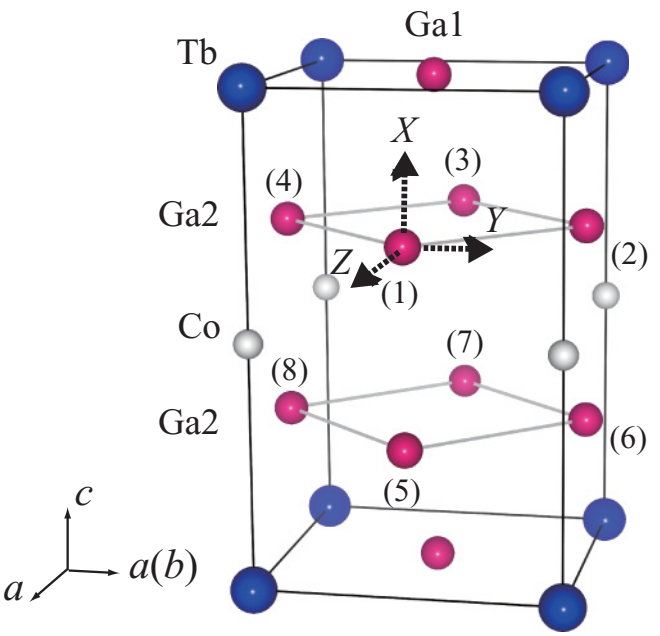

FIG. 1. (Color online) Crystal structure of $TbCoGa_5$. There are two inequivalent Ga sites called Ga1 on top or bottom of the unit cell and Ga2 on the vertical faces. The local principal axes for the EFG at Ga2 (1) are indicated as X, Y, and Z. The local principal axes at Ga2 (2), (3), and (4) are obtained by successive $\pi/4$ rotation of (X,Y,Z) along the c direction. V_{XX}, V_{YY}, and V_{ZZ} correspond to the X, Y, and Z axes, respectively. The numbering shown for Ga2 sites is for discussion in the text.

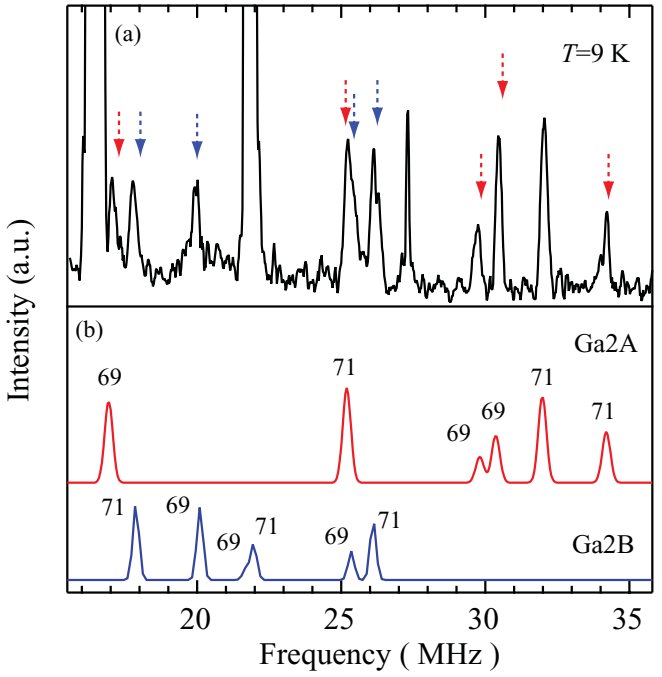

FIG. 2. (Color online) (a) ^{69,71}Ga AFNMR spectrum at 9 K (AF-I phase). Arrows indicate the peak assignments to Ga2 sites in $TbCoGa_5$. (b) Simulated spectra for the Ga2A and Ga2B sites. The simulated spectra are convoluted with a Gaussian function having a natural width of ~150 kHz. The EFG parameters and internal fields for each site are summarized in Table I.

more than 30 μs, where τ is the time between the excitation pulse and the refocusing pulse. The peaks also show relatively large frequency shifts with temperature. Although we used the shortest possible τ of 10 μs in this work, the signals from the Ga2 sites were detected only below 20 K, owing to further shortened T_2 values near T_{N1}. The other peaks in Fig. 2 probably arise from an unknown impurity phase including Ga nuclei. The latter peaks have much longer T_2 and exhibit no frequency shift with temperature, thus were easily distinguishable from the Ga2 peaks. Note that the volume of the impurity phase is not very large. In the AF-II phase, where the intensity of Ga2 peaks recovers dramatically with an ordinary T_2 value, the intensity of the impurity peaks becomes negligibly small in comparison.

Next, in order to extract the EFG parameters ($^{69,71}\nu_Q$ and η) and the internal fields ($H_{\rm int}$) at the Ga2 sites from the AFNMR spectra, we have performed numerical simulation using a diagonalized total Hamiltonian matrix, which consists of the NQR Hamiltonian and a Zeeman term coming from the internal field ($\gamma_N \hbar \boldsymbol{I} \cdot \boldsymbol{H}_{\rm int}$). In the simulation, $^{69}\nu_Q$, η, and $^{69}H_{\rm int}$ are fitting parameters, while $^{71}\nu_Q$ and $^{71}H_{\rm int}$ are calculated from $^{69}\nu_Q$ and $^{69}H_{\rm int}$ using the known ratios $^{69}Q/^{71}Q$ and $^{69}\gamma/^{71}\gamma$, respectively. We found that the spectrum in the AF-I phase is well reproduced as a superposition of spectra from two inequivalent Ga2 sites; these have the same EFG parameters but different internal fields. The $H_{\rm int}$ appears parallel to X for one of the Ga2 sites and parallel to Y for the other. For later discussion, we label them as Ga2A and Ga2B, respectively. The values of EFG parameters and $H_{\rm int}$ so obtained are summarized in Table I.

In Fig. 3, we show the AFNMR spectrum in the AF-II phase. Below T_{N2}, the peaks from the Ga2B suddenly disappear and then reappear at different positions at lower temperatures. The spectrum in the AF-II phase now consists of peaks from three inequivalent Ga sites, Ga2A, $Ga2B^+$, and $Ga2B^-$. The peaks from the Ga2A sites occupy similar positions above and below T_{N2}, indicating that their EFG parameters and the $H_{\rm int}$ are almost the same as those in the AF-I phase, as shown in Table I. On the other hand, the $Ga2B^+$ and the $Ga2B^-$ sites have the same EFG parameters, but different magnitudes for the $H_{\rm int}$. $H_{\rm int}$ is enhanced at the $Ga2B^+$ site, while it is diminished at the $Ga2B^-$ site below T_{N2}, although the orientation of $H_{\rm int}$ remains parallel to Y for both sites.

Finally, to confirm the directions of the EFG tensor axes, we have measured a field-swept NMR spectrum by applying an external field ($H_{\rm ext}$) parallel to the c axis on a single crystal. Figure 4 shows the NMR spectrum obtained at 1.5 K. The spectrum consists of the sets of NMR peaks from Ga1, Ga2A(P), Ga2A(AP), $Ga2B^{+,-}$, and Co sites. The large splitting of the Ga2A is due to the $H_{\rm int}$ along the $H_{\rm ext}$. The Ga2A(P) and the Ga2A(AP) are the sites where the $H_{\rm int}$ appears parallel and antiparallel to the $H_{\rm ext}$. The separation between the Ga2A(P) and the Ga2A(AP) corresponds to $2H_{\rm int} \sim 48$ kOe, and thus $H_{\rm int} \sim 24$ kOe. This gives good agreement with the value estimated from the AFNMR (Table I) and, further, corroborates our choice of the directions of the EFG tensor axes. For the Ga1 and the Co sites, the sets of NMR

TABLE I. EFG parameters and internal fields at Ga2 sites at 9 K (AF-I phase) and 1.5 K (AF-II phase).

	AFM I (9 K)		AFM II (1.5 K)		
	Ga2A	Ga2B	Ga2A	$Ga2B^+$	$Ga2B^-$
$^{69}\nu_Q$ (MHz)	26.44		26.55	26.40	
$^{71}\nu_Q$ (MHz)	16.70		16.77	16.55	
η	0.44		0.45	0.435	
$H_{\rm int}$ (kOe)	22.9 ($\|V_{XX}$)	11.6 ($\|V_{YY}$)	23.3 ($\|V_{XX}$)	19.6 ($\|V_{YY}$)	2.3 ($\|V_{YY}$)

peaks provide $^{69}\nu_Q = 12.17$ MH and $^{71}\nu_Q = 7.68$ MHz with $\eta = 0(V_{ZZ} \parallel c)$, and $^{59}\nu_Q = 0.542$ MHz with $\eta = 0(V_{ZZ} \parallel c)$, respectively. Cancellations of the internal field at both the Ga1 and the Co sites coincide with the propagation vector $\boldsymbol{q} = \langle 1/2,0,1/2\rangle$. Details of the NMR studies on the single crystal will be described in a separate paper.

III. DISCUSSION

Now we proceed to identify magnetic structures based on the AFNMR results. The splitting of the Ga2 in the AF-I phase indicates a break of the tetragonal rotation axis in the AF-I phase, and thus is coincident with the propagation vector obtained from ND measurements.[10] This propagation vector induces an order in a stripe fashion in the ab plane (i.e., TbGa plane). If the propagation vector is of the form $[1/2,1/2,z]$ or $[0,0,z]$, the magnetic structure does not break the tetragonal rotation axis, and thus there is no splitting of Ga2 NMR spectra under zero field.[11–14] With the propagation vector $\boldsymbol{q} = \langle 1/2,0,1/2\rangle$, we can construct five basic models of AF structure based on a representational analysis of the crystallographic space group $P4/mmm$, assuming all the Tb^{3+} ions carry the same moment (i.e., no spin-density wave).[10] Figure 5 shows the five structural models, where thin arrows represent Tb moments. The moments order along the c axis for model (A), while along the a and b axes for models (B) and (D), and models (C) and (E), respectively. Further, the propagation vector is $\boldsymbol{q} = [1/2,0,1/2]$ for models (A), (B), and (C), while it is $\boldsymbol{q} = [0,1/2,1/2]$ for (D) and (E), respectively.

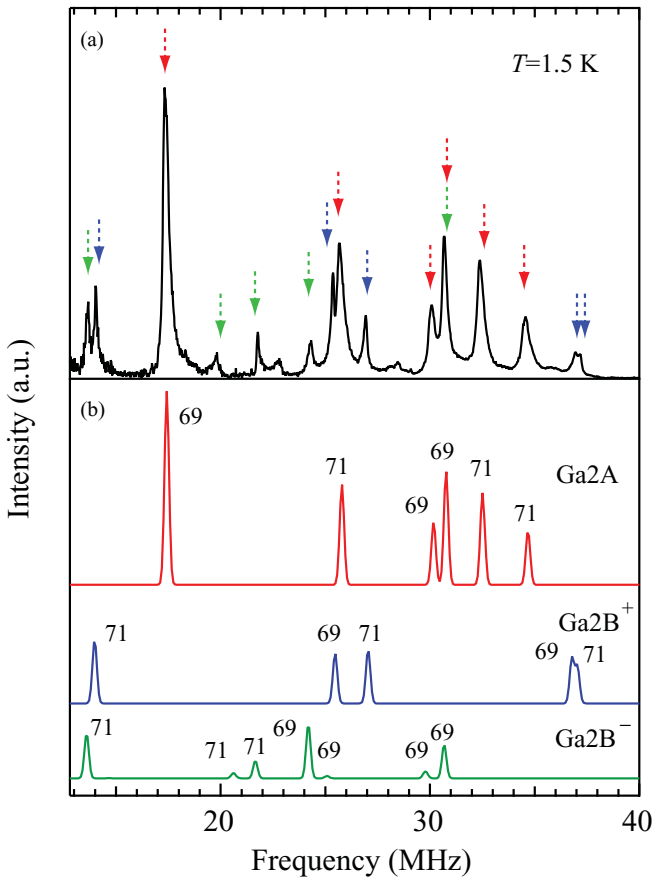

FIG. 3. (Color online) (a) ^{69,71}Ga AFNMR spectrum at 1.5 K (AF-II phase). Arrows indicate the assigned peaks to Ga2 sites. (b) Simulated spectra for Ga2A, $Ga2B^+$, and $Ga2B^-$ sites. The simulated spectra are convoluted with a Gaussian function having a natural width of ~150 kHz. The EFG parameters and internal fields for each site are also summarized in Table I.

A. Symmetry analysis of internal fields

The internal fields at nonmagnetic ligand sites originate from the spin-density distribution of magnetic ions through the dipolar and transferred hyperfine (HF) interactions. The

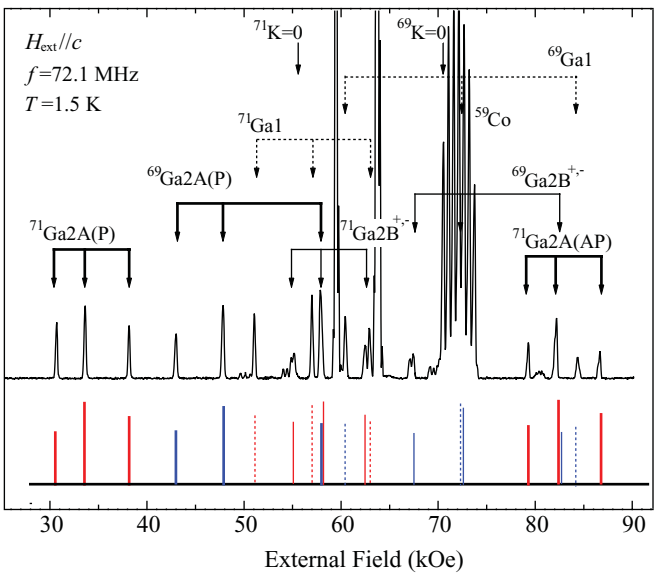

FIG. 4. (Color online) Field-swept NMR spectrum obtained by applying an external field parallel to the c axis on a single crystal of $TbCoGa_5$. In the figure, we also show the result of numerical simulation for ^{69,71}Ga nuclei performed using a diagonalized total Hamiltonian matrix.

TABLE II. HF fields on the Ga2 sites for model (A) described with $m = [0,0,m_z]$ with $\boldsymbol{q} = [1/2,0,1/2]$.

	Model (A)	
	Ga2A (1,3,5,7)	Ga2B (2,4,6,8)
h_Z	0	0
h_Y	0	$\pm 2c_{12}m_z$
h_X	$\pm 2c_{31}m_z$	0

transferred HF interaction arises from the orbital hybridization effect. Evaluating such an effect would require a complete solution to the quantum chemistry of the hybridization process, which is not available. However, even without the complete solution, we can deduce possible directions for the internal field at a nonmagnetic ligand site on the basis of symmetry analysis.[11,13,15] The induced magnetic field at a ligand site never breaks the symmetry of the magnetic sublattice.[15]

From the symmetry analysis, one can construct an invariant form for HF interactions at each ligand site.[16–19] For Ga2 sites in the 115 structure, the invariant form of HF interactions has been derived by Kiss and Kuramoto.[19] Using their invariant form, we have deduced the possible directions of the internal field on the Ga2B for the five structural models. The results obtained are represented by fat arrows in Fig. 5.

Then, by comparing the results with the experimental observations, we can conclude that the magnetic structure corresponds to model (A) for the AF-I phase. Table II summarizes the HF fields derived using the invariant form of the HF interactions for model (A). Here, h_X, h_Y, and h_Z denote the internal fields induced along the local principal axes X, Y, and Z for each Ga2 site, respectively. The c_{ij} are independent constants, which are not determined by the symmetry alone.[19] The arrangement of the Ga2(1)–(8) sites is shown in Fig. 1. As shown in the table, the Ga2 sites split into two inequivalent sites; $H_{\rm int}$ appears parallel to X at the Ga2A [Ga2(1,3,5,7)], while parallel to the Y at the Ga2B [Ga2(2,4,6,8)]. These findings are consistent with experiment.

A splitting of the Ga2 sites is also expected for the other structural models; however, these models do not correspond to experiment. As seen in Fig. 5, models (B) and (E) induce fields $H_{\rm int}$ parallel to X and Z, despite the fact that the $H_{\rm int}$ lie parallel to X and Y in the experiment. On the other hand, models (C) and (D) require that one of the Ga2 sites must have $H_{\rm int} = 0$, but experimentally this is not the case. Thus we can conclude that the ordered structure of the AF-I phase corresponds to model (A).

For the AF-II phase, the propagation vector is still $\boldsymbol{q} = \langle 1/2,0,1/2\rangle$,[10] and thus we consider four mixed models: (A) + (B), (A) + (C), (A) + (D), and (A) + (E).[10] The first two models form collinear structures described with a single propagation vector $\boldsymbol{q} = [1/2,0,1/2]$, while the latter two models result in noncollinear structures described with double propagation vectors $\boldsymbol{q_1} = [1/2,0,1/2]$ and $\boldsymbol{q_2} = [0,1/2,1/2]$. Tables III and IV present the induced HF fields for these four models. We have found that the additional splitting of the Ga2 sites occurs only for the latter two models, namely, the splitting is associated with the second propagation vector $\boldsymbol{q_2}$. Furthermore, this splitting occurs at the Ga2B for model (A) + (D), while it is at the Ga2A for model (A) + (E). The experimental data require a splitting at the Ga2B, keeping the Ga2A equivalent, and thus the only possible solution is model (A) + (D).

TABLE III. HF fields on the Ga2 sites for models (A) + (B) and (A) + (C). The models are described with $m = [m_x,0,m_z]$ and $[0,m_y,m_z]$ with a single propagation vector $\boldsymbol{q} = [1/2,0,1/2]$, respectively.

	Model (A) + (B)		Model (A) + (C)	
	Ga2A (1,3,5,7)	Ga2B (2,4,6,8)	Ga2A (1,3,5,7)	Ga2B (2,4,6,8)
h_Z	$\pm 2c_{21}m_x$	0	0	0
h_Y	0	$\pm 2c_{12}m_z$	$\pm 2c_{11}m_y$	$\pm 2c_{12}m_z$
h_X	$\pm 2c_{31}m_z$	$\pm 2c_{32}m_x$	$\pm 2c_{31}m_z$	0

For model (A) + (D), an a component of the Tb moments appears newly in the AF-II phase. The contribution from the a component is canceled out on the Ga2A, while it induces an additional internal field of $2c_{11}m_x$ on the Ga2B sites, as seen in Table IV. This additional internal field enhances the total $H_{\rm int}$ to become $2(c_{12}m_z + c_{11}m_x)$ at the Ga2B$^+$, while it reduces $H_{\rm int}$ to become $2(c_{12}m_z - c_{11}m_x)$ on Ga2B$^-$ (here, $2c_{12}m_z$ corresponds to $H_{\rm int}$ in the AF-I phase). These are all consistent with the experimental observations, and thus we can conclude the ordered structure in the AF-II phase to be model (A) + (D). The ordered structures obtained for the AF-I and AF-II phases are shown in Fig. 6.

In Fig. 7, we show the temperature dependence of $H_{\rm int}$ for the Ga2A. As shown in Tables II and IV, this $H_{\rm int}$ reflects only the c component of the Tb moment ($=2c_{31}m_z$) in both the AF-I and AF-II phases, since the a component in the AF-II phase is canceled out at the Ga2A. As seen in the figure, $H_{\rm int}$ increases gradually and smoothly with decreasing temperature, and there is no anomaly at $T_{\rm N2}$. In the same temperature region, the ND data indicate that the total value of the Tb moment increases rapidly below $T_{\rm N2}$.[10] This discrepancy between the AFNMR and ND results tells us that the a component of the Tb moment develops without changing the value of the c component below $T_{\rm N2}$. This result is supportive of the successive components-separated phase transitions proposed for this compound.[9,10]

B. EFG parameters in the AF ordered states

Concerning the EFG parameters ν_Q and η, all of the Ga2 sites remain equivalent in the AF-I phase, although they are split into the Ga2A and the Ga2B by $H_{\rm int}$. They only develop inequivalent EFG parameters below $T_{\rm N2}$. This behavior can be understood in terms of the quadrupolar HF interactions ascribed to Tb $4f$ electrons. For the 115 structure, an invariant form of the quadrupole HF interaction has also been derived in a previous paper.[19]

In the AF-I phase, the ordering of the dipoles along the c axis (J_z) induces homogeneous O_{02} quadrupoles, even if there is no interatomic quadrupolar interaction among them. However, the quadrupole moment $\langle O_{02}\rangle$ is nonzero even in the paramagnetic state because of the tetragonal symmetry of

TABLE IV. HF fields on the Ga2 sites for models (A) + (D) and (A) + (E). The models are described with $m = [m_x,0,m_z]$ and $[0,m_y,m_z]$ with double propagation vectors $\boldsymbol{q_1} = [1/2,0,1/2]$ and $\boldsymbol{q_2} = [0,1/2,1/2]$.

	Model (A) + (D)			Model (A) + (E)		
	Ga2A (1,3,5,7)	Ga2B$^+$ (2,8)	Ga2B$^-$ (4,6)	Ga2A$^+$ (1,7)	Ga2A$^-$ (3,5)	Ga2B (2,4,6,8)
h_Z	0	0	0	0	0	$\pm 2c_{21}m_y$
h_Y	0	$\pm 2(c_{12}m_z + c_{11}m_x)$	$\pm 2(c_{12}m_z - c_{11}m_x)$	0	0	$\pm 2c_{12}m_z$
h_X	$\pm 2c_{31}m_z$	0	0	$\pm 2(c_{31}m_z + c_{32}m_y)$	$\pm 2(c_{31}m_z - c_{32}m_y)$	0

the crystal. Therefore, the EFG parameters derived from the homogeneous O_{02} moments never split the Ga2 NMR spectra, consistent with experimental results. The uniformity of the EFG tensors at the Ga2 sites also ensures that the tetragonal symmetry of the crystal is still preserved in the AF-I phase, even though the ordered structure breaks the tetragonal rotation axis.

With dipolar order $\langle J_z \rangle \neq 0$, the local symmetry is reduced to C_{2v} from D_{4h}.[19] Within the C_{2v} symmetry, the dipoles $\langle J_x \rangle$ mix with the quadrupoles O_{zx} in the same irreducible representation. Thus the ordering of $\langle J_x \rangle$ in the AF-II phase induces a homogeneous quadrupole component O_{zx}. From the invariant form of the quadrupolar HF interaction, we know that the O_{zx} induces nonzero values for the EFG tensor components of V_{ZX} and V_{XY} for the Ga2A and the Ga2B, respectively. Therefore, the EFG parameters can be inequivalent between these two sites. (The Ga2B$^+$ and the Ga2B$^-$ are equivalent for the O_{zx}, as observed also in the experimental results.)

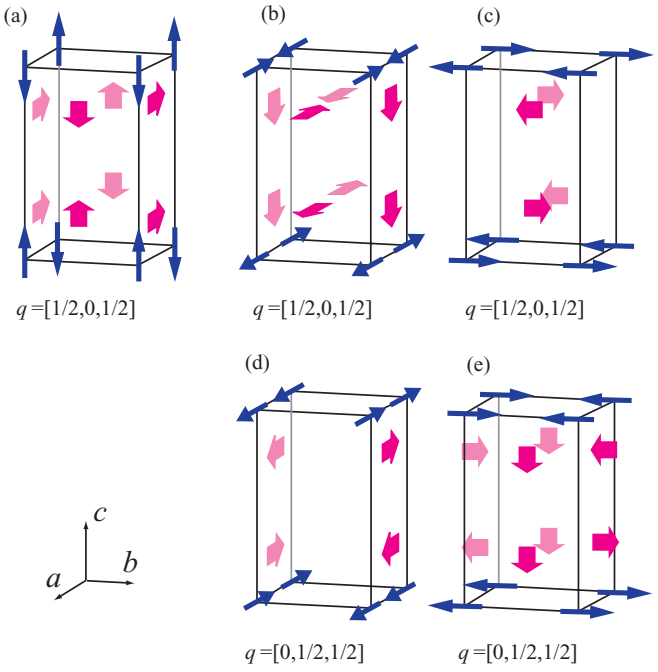

FIG. 5. (Color online) Models for the AF structure of $TbCoGa_5$ developed on the basis of ND results. The thin arrows denote the magnetic dipole moments of the Tb ions. The fat arrows indicate the HF field at Ga2 sites.

C. Magnetic interactions

Now we discuss magnetic interactions in $TbCoGa_5$. As shown in Fig. 6, the Tb moments order in a stripe fashion on the square TbGa lattice in the AF-I phase. In the square lattice, however, the stripe order is not stabilized with nearest-neighbor couplings alone. One is required to include both nearest-neighbor J_1 (along the side of the square) and next-nearest-neighbor J_2 (along the diagonal) antiferromagnetic interactions. Such a frustrated J_1-J_2 model has been studied intensively for the two-dimensional Heisenberg antiferromagnet on a square lattice.[20] These studies have shown that the Néel order of the pure J_1 model is stabilized for $J_2/J_1 \ll 0.5$, while the stripe order is established for $J_2/J_1 \gg 0.5$. In the TbGa plane, we expect $J_1 \approx J_2$, since effective magnetic interactions would be mediated via Ga1 orbitals, which are located at the centers of the lattice squares.

It is also likely that such an in-plane frustration is responsible for the emergence of the noncollinear magnetic structure in the AF-II phase. In general, a noncollinear structure occurs to reduce the extent of magnetic frustration, and hence is often observed in a compound with geometric frustration. In the 115 structure, there is no geometric frustration, but we can expect a measure of in-plane magnetic frustration by the mechanism mentioned above. Of course, the actual situation would be more complicated. A possible occurrence of frustration phenomena caused by the competition between dipolar and quadrupolar interactions has been discussed

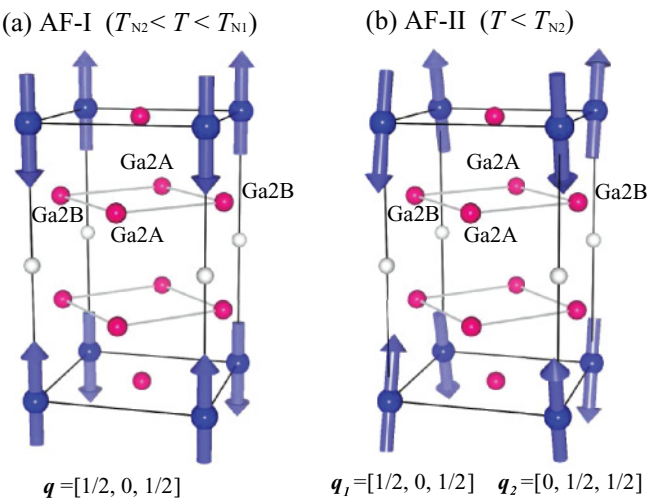

FIG. 6. (Color online) Magnetic structures for (a) the AF-I and (b) the AF-II phases, respectively.

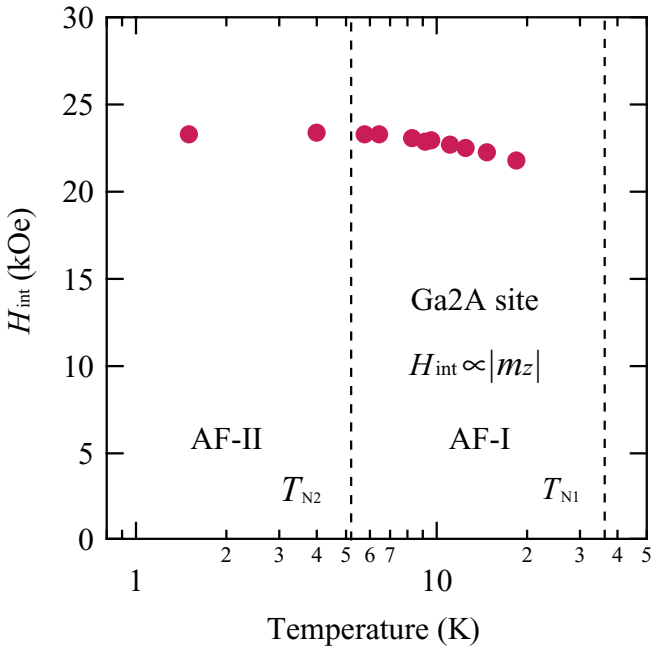

FIG. 7. (Color online) Temperature dependence of H_{int} at the Ga2A sites. This value is proportional to the c component of the Tb moment in both the AF-I and AF-II phases.

for this compound.[8,9] As for successive transition behaviors observed in Np115 systems,[13,21–25] the importance of quadrupolar interactions has been noted in the theoretical papers.[19,26,27] In addition, the intra-atomic interactions, such as the crystal-field effect and spin-orbit coupling, would also be important. Further experimental and theoretical efforts are needed to understand the complex magnetism of this system.

IV. SUMMARY

From analysis of the internal fields at Ga2 sites, we have determined the magnetic structures of the AF-I and the AF-II phases of $TbCoGa_5$. The AF-I phase is a collinear AF order with the propagation vector $\boldsymbol{q} = [1/2,0,1/2]$ and with ordered moments parallel to the c axis. This is in accordance with the ND measurements. In the AF-II phase, on the other hand, we found a noncollinear AF structure described with double propagation vectors $\boldsymbol{q_1} = [1/2,0,1/2]$ and $\boldsymbol{q_2} = [0,1/2,1/2]$. Interestingly, the AFNMR reveals that the c component of the Tb moments does not change value between the AF-I and the AF-II phases, even though an a component is newly developed in the AF-II phase. The EFG parameters indicate the appearance of a homogeneous quadrupole component O_{zx} in the AF-II phase.

In 115 systems, a surprisingly wide variety of ordered structures has been discovered for this single-crystal structure.[13,23,24,28–30] The richness of their magnetic structures implies that their intra- and interatomic interactions are rather complex. We suggest that these complexities may arise in part from the frustrated magnetism hidden in the square plane lattice.

ACKNOWLEDGMENTS

We thank K. Kubo, K. Kaneko, and R. E. Walstedt for valuable discussions and comments. A part of this work was supported by a Grant-in-Aid for Scientific Research on Innovative Areas “Heavy Electrons”(No. 20102006 and No. 20102007) by the Ministry of Education, Culture, Sports, Science and Technology of Japan. One of the authors (N.S.) acknowledges the support from the Research Fellowship of Japan Society for the Promotion of Science (JSPS) for Young Scientists.

*tokunaga.yo@jaea.go.jp

[1]For a review, see, e.g., J. L. Sarrao and J. D. Thompson, J. Phys. Soc. Jpn. **76**, 051013 (2007).
[2]H. Hegger, C. Petrovic, E. G. Moshopoulou, M. F. Hundley, J. L. Sarrao, Z. Fisk, and J. D. Thompson, Phys. Rev. Lett. **84**, 4986 (2000).
[3]C. Petrovic, P. G. Pagliuso, M. F. Hundley, R. Movshovich, J. L. Sarrao, J. D. Thompson, Z. Fisk, and P. Monthoux, J. Phys. Condens. Matter **13**, L337 (2001).
[4]J. L. Sarrao, L. A. Morales, J. D. Thompson, B. L. Scott, G. R. Stewart, F. Wastin, J. Rebizant, P. Boulet, E. Colineau, and G. H. Lander, Nature (London) **420**, 297 (2002).
[5]F. Wastin, P. Boulet, J. Rebizant, E. Colineau, and G. H. Lander, J. Phys. Condens. Matter **15**, S2279 (2003).
[6]J. Hudis, R. Hu, C. L. Broholm, V. F. Mitrovic, and C. Petrovic, J. Magn. Magn. Mater. **307**, 301 (2006).
[7]Yu. N. Grin’, Ya. P. Yarmolyuk, and E. I. Gladyshevskii, Kristallografiya **24**, 242 (1979).
[8]N. Sanada, T. Muneoka, R. Watanuki, K. Suzuki, M. Akatsu, and T. Sakakibara, J. Phys.: Conf. Ser. **150**, 042172 (2009).
[9]N. Sanada, R. Watanuki, K. Suzuki, M. Akatsu, and T. Sakakibara, J. Phys. Soc. Jpn. **78**, 073709 (2009).
[10]R. Watanuki, N. Sanada, K. Suzuki, J. van Duijn, and G. Andre, J. Phys. Soc. Jpn., Suppl. A **80**, SA083 (2011).
[11]T. Ohama, M. Hirano, and S. Noguchi, Phys. Rev. B **71**, 094408 (2005).
[12]H. Sakai, S. Kambe, Y. Tokunaga, T. Fujimoto, R. E. Walstedt, H. Yasuoka, D. Aoki, Y. Homma, E. Yamamoto, A. Nakamura, Y. Shiokawa, and Y. Ōnuki, Phys. Rev. B **76**, 024410 (2007).
[13]S. Kambe, H. Sakai, Y. Tokunaga, R. E. Walstedt, D. Aoki, Y. Homma, and Y. Shiokawa, Phys. Rev. B **76**, 144433 (2007).
[14]R. E. Walstedt, S. Kambe, Y. Tokunaga, and H. Sakai, J. Phys. Soc. Jpn. **76**, 072001 (2007).
[15]S. Demuynck, L. Sandratskii, S. Cottenier, J. Meersschaut, and M. Rots, J. Phys. Condens. Matter **12**, 4629 (2000).
[16]O. Sakai, R. Shiina, H. Shiba, and P. Thalmeier, J. Phys. Soc. Jpn. **66**, 3005 (1997).
[17]O. Sakai, R. Shiina, and H. Shiba, J. Phys. Soc. Jpn. **74**, 457 (2005).
[18]O. Sakai, J. Kikuchi, R. Shiina, H. Sato, H. Sugawara, M. Takigawa, and H. Shiba, J. Phys. Soc. Jpn. **76**, 024710 (2007).
[19]A. Kiss and Y. Kuramoto, J. Phys. Soc. Jpn. **77**, 124708 (2008).
[20]For a review, see, e.g., E. Manousakis, Rev. Mod. Phys. **63**, 1 (1991).

[21]D. Aoki, Y. Homma, Y. Shiokawa, H. Sakai, E. Yamamoto, A. Nakamura, Y. Haga, R. Settai, and Y. Ōnuki, J. Phys. Soc. Jpn. **74**, 2323 (2005).
[22]N. Metoki, J. Phys. Soc. Jpn., Suppl. **75**, 24 (2006).
[23]F. Honda, N. Metoki, K. Kaneko, S. Jonen, E. Yamamoto, D. Aoki, Y. Homma, Y. Haga, Y. Shiokawa, and Y. Ōnuki, Phys. Rev. B **74**, 144413 (2006).
[24]S. Jonen, N. Metoki, F. Honda, K. Kaneko, E. Yamamoto, Y. Haga, D. Aoki, Y. Homma, Y. Shiokawa, and Y. Ōnuki, Phys. Rev. B **74**, 144412 (2006).
[25]E. Colineau, J. P. Sanchez, F. Wastin, P. Boulet, and J. Rebizant, J. Phys. Condens. Matter **19**, 246202 (2007).
[26]H. Onishi and T. Hotta, New J. Phys. **6**, 193 (2004).
[27]A. Kiss and Y. Kuramoto, J. Phys. Soc. Jpn. **75**, 034709 (2006).
[28]Y. Tokiwa, Y. Haga, N. Metoki, Y. Ishii, and Y. Ōnuki, J. Phys. Soc. Jpn. **71**, 725 (2002).
[29]K. Kaneko, N. Metoki, N. Bernhoeft, G. H. Lander, Y. Ishii, S. Ikeda, Y. Tokiwa, Y. Haga, and Y. Ōnuki, Phys. Rev. B **68**, 214419 (2003).
[30]N. Metoki, K. Kaneko, E. Colineau, P. Javorsky, D. Aoki, Y. Homma, P. Boulet, F. Wastin, Y. Shiokawa, N. Bernhoeft, E. Yamamoto, Y. Ōnuki, J. Rebizant, and G. H. Lander, Phys. Rev. B **72**, 014460 (2005).